Biocatalysis and Agricultural Biotechnology 18 (2019) 101047

Contents lists available at ScienceDirect

Biocatalysis and Agricultural Biotechnology

journal homepage: www.elsevier.com/locate/bab

Identification of *Bacillus thuringiensis* bacterial strain isolated from the mine soil as a robust agent in the biosynthesis of silver nanoparticles with strong antibacterial and anti-biofilm activities

Moj Khaleghi[a,*], Sadegh Khorrami[b], Hadi Ravan[a]

[a] Department of Biology, Faculty of Sciences, Shahid Bahonar University of Kerman, Kerman, Iran
[b] Department of Biotechnology, Faculty of Advanced Sciences and Technologies, University of Isfahan, Isfahan, Iran

ARTICLE INFO

Keywords:
Antibacterial agent
Anti-biofilm agent
Bacillus thuringiensis
Mine soil
Silver nanoparticles

ABSTRACT

Biofilm formation is one of the major problems associated with pathogenic bacteria besides drug resistance. In this study, the potential of the bacterial strain of mine soil in the biosynthesis of silver nanoparticles with antibacterial and anti-biofilm activities was investigated. The study revealed that the isolated *Bacillus thuringiensis* is an efficient bacterial strain in the biosynthesis of silver nanoparticles. Based on the results, the spherical biosynthesized silver nanoparticles with a 42 nm average size have good antibacterial properties at low concentrations (MIC = 6.25–12.5 μg/mL). Moreover, these nanoparticles not only inhibited the formation of biofilm, but were also able to interfere in biofilm metabolic activity and its degradation. Besides, with increasing concentrations of nanoparticles, degeneration of bacterial biofilm also increased so that the highest rate of bacterial biofilm degeneration (> 90%) was observed at 6 μg/mL concentration.

1. Introduction

Nowadays, besides the issue of drug resistance, one of the major problems associated with pathogenic bacteria is the formation of biofilm, an organized community of bacteria adherent to a surface. It contains an extracellular polymeric substance made of exopolysaccharides and nucleic acids, retains the nutrients, and protects the cell from antimicrobial agents (Yahyaei and Pourali, 2017). Biofilm expansion has been introduced as the leading cause of nosocomial infections and 80% of human infections because these bacteria not only are protected against different types of antibiotics and other environmental stresses, but also escape from the host immune response; hence, biofilm increases bacterial dispersion and pathogenesis. It is said that killing the bacteria in a biofilm matrix requires 1000 times as much antibiotics as compared to planktonic cells (Dufour et al., 2012; Singh et al., 2015). Therefore, there is an urgent need to search for a cost-effective and more efficient strategy for a combating bacterial biofilm.

Using products of nanotechnology is one of the promising approaches to eliminating bacterial biofilm. Nowadays, nanomaterials are widely used in various industries. Among different types of nanomaterials, nanoparticles, especially silver nanoparticles, have attracted special attention because of their unique physicochemical properties. Moreover, anti-oxidant, anti-fungal, anti-cancer and anti-microbial features are the most relevant aspects of silver nanoparticles. In addition, the anti-biofilm behavior of these nanoparticles has recently been reported in some cases (Deljou and Goudarzi, 2016; Mostaghasi et al., 2018; Prasad et al., 2007; Singh et al., 2015).

Currently, physical, chemical, and particularly biological methods are being used in the synthesis of nanoparticles. Among them, biological methods have recently received more attention because they are nontoxic, eco-friendly, bio-safe, and relatively easier to synthesize at ambient conditions (Deljou and Goudarzi, 2016; Singh et al., 2015). Nanoparticles can be synthesized from multicellular organisms like plants to unicellular ones like bacteria (Das et al., 2014; Natarajan et al., 2010; Nithya and Ragunathan, 2009; Pourali and Yahyaei, 2016). Depending on microorganism features, this can be done intracellularly or extracellularly; however, extracellular synthesis of metallic nanoparticles by the microorganism is simpler and more economical (Abd El- Aziz et al., 2012; Kalishwaralal et al., 2010b; Shahverdi et al., 2007). Search for a robust microorganism in the biosynthesis of desirable nanoparticles, as the interface of microbiology and nanotechnology, is continuing.

In this study, the biosynthesis of silver nanoparticles (AgNPs) was investigated using isolated bacterial strains from the soil of Sirjan Gol-Gohar Mine located in Kerman Province, Iran. In addition, antimicrobial properties of synthesized AgNPs against some pathogenic

* Corresponding author.
E-mail address: m.khaleghi@uk.ac.ir (M. Khaleghi).

https://doi.org/10.1016/j.bcab.2019.101047
Received 11 December 2018; Received in revised form 31 January 2019; Accepted 13 February 2019
Available online 14 February 2019
1878-8181/

bacteria were investigated. Moreover, the inhibitory effect of these AgNPs on bacterial biofilm formation and the effect of their removal on pre-formed biofilm were evaluated. Biofilm destruction was achieved using microtiter plate and staining with crystal violet (CV) because CV is suitable for the evaluation of biofilm amount, not for the examination of its activity (Pitts et al., 2003). In this research, respiratory dye, triphenyl tetrazolium chloride (TTC), was also used to measure the active metabolism of bacteria.

2. Materials and methods

2.1. Isolation of bacterial strains

Soil samples were collected at 5 cm depth from Sirjan Gol-Gohar Mine located in Kerman, Iran. They were taken to the laboratory in sealed sterile containers, and serial dilutions were prepared for each collected sample. Each dilution was incubated on Nutrient agar bacterial medium culture (Merck, Germany) at 30 °C for 24–48 h. Based on size, color, and shape, each colony was isolated to obtain a pure culture. Then, these colonies were named GL-1 to GL-48 and were stored in 20% glycerol stock solution at −20 °C for future tests.

2.2. Molecular identification

Genomic DNA of GL22 strain, as the best strain in the biosynthesis of nanoparticles, was extracted according to phenol extraction; and its purity was checked by the A260/A280 ratio. Universal 16S rRNA PCR primer sets, including U8F (5′-AGAGTTTGATCCTGGCTCAG-3′) as the forward primer and U1390R (5′-GACGGGCGGTGTGTACAA-3′) as a reverse primer, were used to amplify 16S rRNA gene. The PCR was accomplished in a total volume of 50 µL including 50 ng of genomic DNA, 1.25 Units of Taq DNA polymerase, 20 pmol of each primer, 10x PCR buffer and 200 µM of each dNTPs as components. The PCR was done as follows: for 35 cycles with the primary denaturing for 3 min at 94 °C, recurring denaturing for 30 s at 94 °C, recombining in the double-stranded form for 30 s at 58 °C and extension for 2 min at 72 °C with a final extension of 7 min at 72 °C. PCR products underwent electrophoresis on agarose gel (1%); afterwards, they were amplified 16S rRNA bands, and were purified by DNA extraction kit (Cinaclone, Tehran, Iran, Cat. No.: PR881613). Then, DNA sequencing was directly done on both strands by Bioneer Company (South Korea). The sequence data of 16S rRNA was then used for BLAST analysis, and a phylogenetic tree was made on Molecular Evolutionary Genetics Analysis software (MEGA4) (Tamura et al., 2007).

2.3. Isolation of silver nitrate reducer bacteria

In order to explore the possibility of synthesizing AgNPs using supernatant, each isolated bacterium was separately incubated in 100 mL Luria-Bertani (LB) broth medium at 120 rpm at 30 °C for 48 h. The bacteria were then centrifuged at 8000 rpm for 10 min at 4 °C so that supernatant was collected and filtrated through 0.22 µm filters. Then, the supernatant was added to silver nitrate (5 mM) ($AgNO_3$, Merck, Germany) at 30 °C for 24 h under dark conditions. The bacterial supernatants containing AgNPs were centrifuged at 15000 rpm for 20 min in order to collect AgNPs. The obtained pellets were re-suspended in sterile Phosphate-buffered saline (PBS) and centrifuged again, and this step was repeated three times (Pourali and Yahyaei, 2016; Singh et al., 2016). The obtained AgNPs were then dried overnight at 60 °C, and their properties were examined.

2.4. Evaluation of AgCl precipitate formation

For initial verification of the AgNPs synthesis, pure sodium chloride (NaCl) was added to the color-changed solution containing these nanoparticles at 1:10 (w/v). If the milky-color precipitate of AgCl is not observed, it indicates that all of the silver ions are reduced to AgNPs (Levard et al., 2013).

2.5. Characterization of AgNPs

UV–vis spectrophotometer (Shimadzu, Kyoto, Japan) was applied to record UV-Vis spectrum of the mixture in the range of 300–700 nm. The synthesized AgNPs X-Ray Diffraction (XRD) spectrum (30–80° in 2θ) was recorded by Bruker, Madison, USA, X-ray Diffractometer at a voltage of 40 kV and a current of 30 mA with CuKα X-ray source.

The size distribution and morphology of AgNPs were determined using field emission scanning electron microscopy FE-SEM (JEOL JSM 6700F, Germany) and transmission electron microscopy (TEM) (Zeiss-CEM-902A, Germany). The AgNPs were also analyzed using EDX-spectroscopy (by the same instrument).

In this study, the stability of the biosynthesized AgNPs was examined by keeping the reaction mixture at room temperature for 3 months, and it was evaluated by UV–vis spectroscopy in the range of 300–700 nm (Anjum and Abbasi, 2016; Singh et al., 2016).

2.6. Antibacterial activity

In order to determine the antimicrobial activity of synthesized AgNPs, 6 bacterial strains including *Staphylococcus aureus* PTCC 1112, *Escherichia coli* O157H7, *Listeria monocytogenes* PTCC 1298, *Pseudomonas aeruginosa* PTCC 1310, *Klebsiella pneumoniae* PTCC 1053, and *Enterococcus faecalis* PTCC 1237 were purchased from Pasteur Institute of Iran, and they were employed in the study. Antimicrobial activity of synthesized silver nanoparticles was measured using methods of agar well diffusion. For good diffusion, the wells were created on Muller-Hinton Agar (MHA) plates with a sterile cork-borer (6.0 mm diameter). Microbial strains were cultured after achieving a turbidity of a 0.5 McFarland standard on each plate using a sterile swab. Next, 50 µL of (50 µg/mL) of AgNPs solution was poured into each well, and the plates were incubated at 37 °C for 24 h. The inhibition zone diameter (mm) was measured after the incubation period, and the filter-sterilized supernatant without $AgNO_3$ solution was used as negative control. The experiments were done in triplets, and the results were explained in terms of mean standard deviation.

2.7. MIC and MBC of AgNPs

Silver nanoparticles solution was made in sterile 96-well plates by serial two-fold dilution in the range of 0.78–50 µg/mL in order to determine minimum inhibitory concentration (MIC) and minimum bactericidal concentration (MBC). The wells were then inoculated with an overnight culture of pathogenic strains adjusted to 0.5 McFarland, diluted at a 1:100 ratio, and then incubated at 37 °C for 24 h. The mean of live pathogenic cells was recorded using ELISA reader (Bio-Rad Laboratories, Inc., Hercules, CA, USA) at 600 nm. MBC, the lowest concentration of nanoparticles that kills over 99% of the bacteria, was determined by spreading the broth from the non-growth wells onto nutrient agar plates, and was incubated at 37 °C for 24 h. MBC was distinguished based on the concentration without any growth of the pathogenic strains (Balouiri et al., 2016; Khorrami et al., 2018).

2.8. Evaluation of the anti-biofilm activity of AgNPs

2.8.1. Biofilm inhibition

To examine the inhibition of biofilm formation (IBF) effect of AgNPs, Microtiter plate adhesion assay was used. Biofilm formation in this assay was determined using the method reported earlier (Stepanovic et al., 2007) with some modifications. The overnight culture of bacterial strains adjusted to 0.5 McFarland were diluted at the 1:100 ratios in fresh medium in wells of a sterile 96-well microtiter plate. Each well was then inoculated with 100 µL of AgNPs dilution

(0.78–50 μg/mL). As a control, 100 μL of phosphate-buffered saline (PBS) was added to certain wells instead of AgNPs suspension. The plate was incubated for 24 h at 37 °C. After incubation, the media were removed and the wells were washed three times with 200 μL of sterile distilled water. Next, the microtiter plate was kept to be air dried for 45 min. Afterwards, 200 μL of 0.1% (v/v) crystal violet was added to each well and kept for 45 min. The wells were then washed three times with 300 μL of sterile distilled water to remove the extra stain. The dye, combined with the adherent cells, was solubilized with 200 μL of glacial acetic acid 33% (Merck, Germany). The absorbance of each well was measured at 492 nm using a microtiter plate ELISA reader. The percentage of inhibition was calculated according to Equation (1) (Pitts et al., 2003).

$$Inhibition\ percentage = \frac{A_{control} - A_{sample}}{A_{control}} \times 100 \quad (1)$$

$A_{control}$ = absorbance average of the control wells
A_{sample} = absorbance average of the sample wells

2.8.2. Biofilm degeneration

AgNPs ability to eliminate and destroy biofilm structures was evaluated by using microtiter plate according to the method described by Singh et al. (2016) with some modifications. Bacterial suspensions with turbidity of 0.5 McFarland were prepared. 200 μL of each microbial suspension was added into wells, and they were then incubated at 37 °C for 24 h. To examine AgNPs ability to destroy biofilm structure, the media were removed, 200 μL of AgNPs 1–6 μg/mL concentrations were added, and the plates were incubated at 37 °C for 24 h 200 μL of PBS was added to certain wells as a control. After removing the media, the wells were washed three times with 200 μL of sterile water. Then, they were dried at room temperature and stained by crystal violet 0.1%. After removing the extra stain and adding 200 μL of glacial acetic acid 33%, the absorbance of each well was measured at 492 nm. The percentage of biofilm destruction was also determined by Equation (1) (Pitts et al., 2003; Sonak and Bhosle, 1995).

2.8.3. Inhibition of biofilm metabolic activity

Dehydrogenase activity was examined in order to measure the survival rate of biofilms bacteria treated with AgNPs (1–6 μg/mL). The biofilms formed by pathogens in 96-well microtiter plates were treated with 150 μL AgNPs at concentrations of 1–6 μg/mL, and were incubated at 37 °C for 24 h again. 50 μL aliquot of the electron acceptor solution, triphenyltetrazolium chloride (TTC) (0.25 g TTC in 100 mL of tris buffer, pH = 7), was added to each well, and the plates were incubated at 37 °C for 24 h for color change. The OD was measured against a blank at 490 nm (Babu et al., 2012; Bai et al., 2019; Suresh et al., 2016).

2.9. Statistical analyses

The data were exposed to One-way Analysis of Variance (ANOVA) to determine the importance of individual differences at $p < 0.05$ level. Important means were compared by Duncan's multiple range tests. All statistical analyses were performed using SPSS Version 16.

3. Results

3.1. Isolation of silver nitrate reducer bacteria

After preparing serial dilutions and culturing, 48 isolates of different bacterial colonies (GL1-GL48) were obtained. Based on the primary signs, time, color change rate and UV-Vis spectrum of the mixture, GL22 was selected as a favorable strain to reduce silver ions extracellularly at 24 h. Therefore, subsequent studies were conducted on this strain.

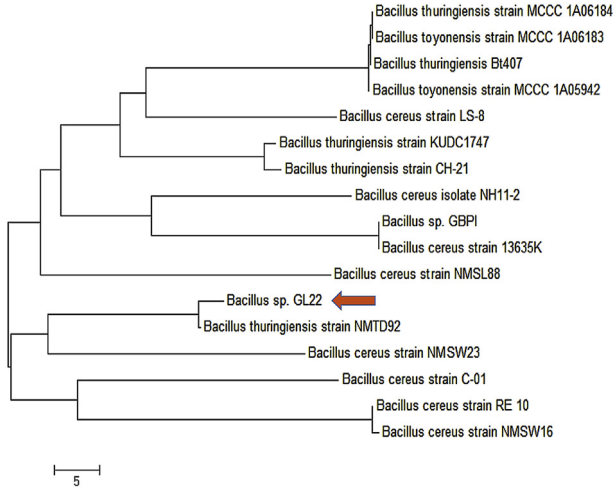

Fig. 1. The phylogenetic tree, based on partial 16S rDNA sequences, represents the relationship between GL22 strain and other species belonging to the genus *Bacillus*. The analysis was constructed using the neighbor-joining method in MEGA4.

3.2. Molecular identification of GL22 strain

The desirable bacterial species were identified by using information obtained by sequencing 16S rRNA gene. The results of sequence alignment and phylogenetic tree revealed that the $AgNO_3$ reducer strain (GL22) was 97% similar to *Bacillus thuringiensis* (Fig. 1).

3.3. AgCl precipitate formation

NaCl was added to the final mixture to confirm the completion of silver ions reduction by bacterial extracellular components. Lack of white precipitate of AgCl indicates that all of the silver ions in the medium were reduced to silver nanoparticles (Levard et al., 2013).

3.4. Characterization of AgNPs

3.4.1. UV-vis spectroscopy

The synthesis of nanoparticles by the isolated *B. thuringiensis* was verified by the color change of mixture from light yellow to dark brown (Fig. 2, b). Fig. 2, a, UV-Vis absorption spectrum of the mixture (300–700 nm), demonstrates an intensive absorption peak at 443 nm related to AgNPs colloid (Khorrami et al., 2018). Results of stability examination of synthesized AgNPs revealed that there was no change in color and UV-Vis absorbance of the mixture, and no deposit was observed.

3.4.2. X-ray diffraction pattern of AgNPs

The XRD spectrum of nanoparticles was recorded in order to characterize their crystal structure. As illustrated in Fig. 3, four distinct diffraction peaks at $2\theta = 38.16°$, 44.63°, 64.48°, and 77.02° appeared, which index the plans (111), (200), (220), and (311) of the cubic face-centered silver crystals. This is closely similar to the announced reference value of International Centre for Diffraction Data (ICDD) number 01-087-0718.

3.4.3. FE-SEM, TEM and EDS analyses of AgNPs

The EDS spectrum (Fig. 4, b) showed the highest peak of Ag at 3 keV, which indicates that the AgNPs were successfully produced by the cell free supernatant of the isolated *B. thuringiensis* strain. FE-SEM images revealed that the morphology of AgNPs is approximately spherical and their average size is 42 ± 7 nm. Moreover, no aggregation was observed in this image. In addition, the TEM analysis result confirms the spherical morphology of nanoparticles (Fig. 5).

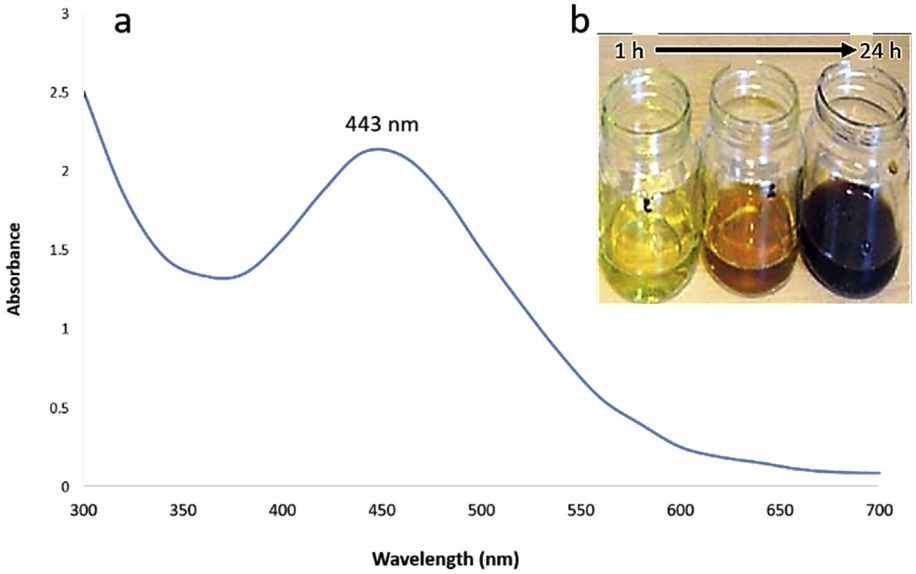

Fig. 2. a, UV-Vis spectrum of biosynthesized AgNPs, and b, color change of the biosynthesized AgNPs mixture during reaction time. (For interpretation of the references to color in this figure legend, the reader is referred to the Web version of this article.)

3.5. Biological aspects of AgNPs

3.5.1. Antibacterial activity of AgNPs

The antimicrobial effect of synthesized AgNPs was explored in six reference microorganisms (including *S. aureus*, *E. coli*, *L. monocytogenes*, *P. aeruginosa*, *K. pneumoniae*, *and E. faecalis*). The results indicated that synthesized AgNPs exhibit a significant antibacterial behavior against all the examined bacterial strains. Inhibition zone diameter (IZD), minimum inhibitory concentration (MIC) and minimum bactericidal concentration (MBC) of the synthesized AgNPs on pathogenic bacteria have been provided in Table 1. The results clearly showed that AgNPs not only inhibited bacterial growth, but also killed them even at low concentrations. The minimum concentration of AgNPs for inhibiting and killing pathogens was around 6.25–25 μg/mL.

3.5.2. Inhibition of biofilm formation and biofilm degeneration

Results of the anti-biofilm examination revealed that these AgNPs could absolutely inhibit biofilm formation in all bacteria at sub-MIC concentration except *L. monocytogenes* (Table 1). Additionally, the results of biofilm degeneration indicate that over 50% of biofilm formed by pathogenic bacteria was eliminated by these AgNPs at 4–6 μg/mL concentrations ($p < 0.001$) so that over 90% of bacterial biofilm was destroyed at the concentration of 6 μg/mL (Fig. 6).

3.5.3. Inhibition of biofilm metabolic activity

The inhibitory function of synthesized AgNPs on metabolic activity of biofilm is shown in Fig. 7. The results showed that the nanoparticles had a remarkable impact on biofilm metabolic activity, which is dose-dependent.

4. Discussion

In this study, although isolated strains were able to synthesize AgNPs both intracellularly and extracellularly, the procedure was continued using extracellular samples because extracellular synthesis method was easier and more economical. However, the exact mechanism of extracellular synthesis of nanoparticles by microorganisms is still unknown. It seems that microorganisms contribute to reducing

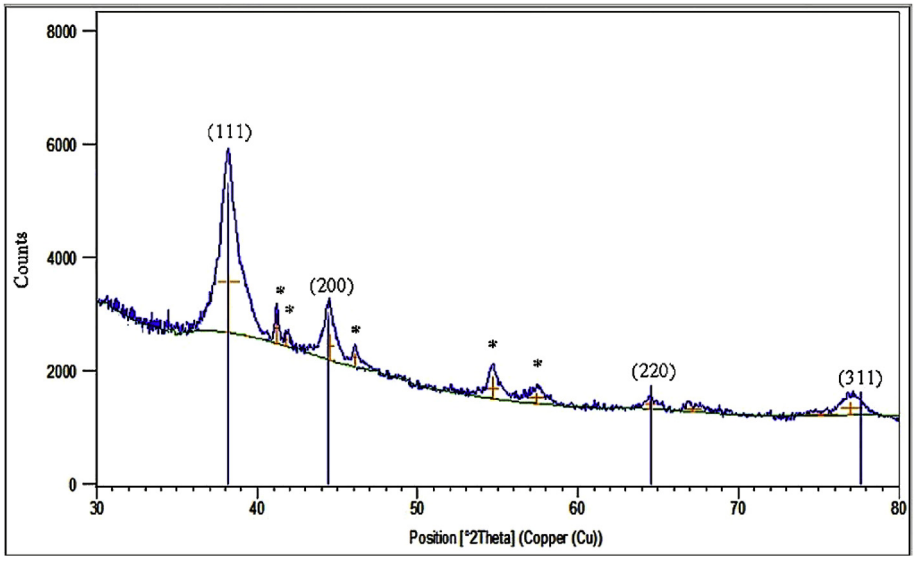

Fig. 3. XRD spectrum of biosynthesized AgNPs.

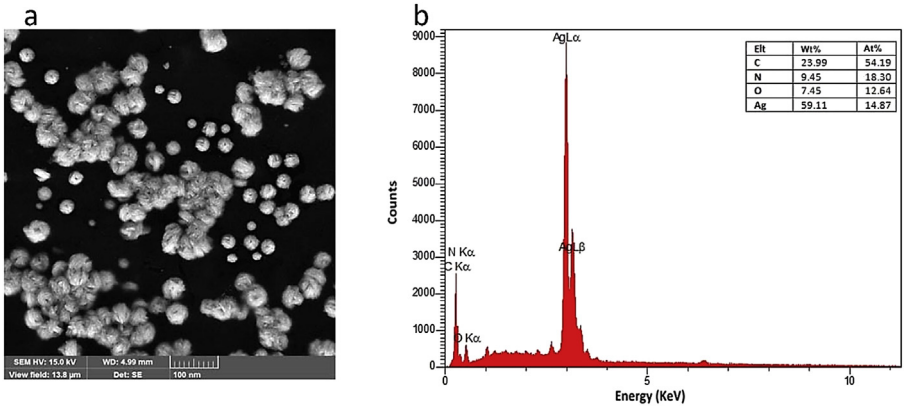

Fig. 4. a, FE-SEM image of biosynthesized AgNPs, and b, EDS spectrum of biosynthesized AgNPs.

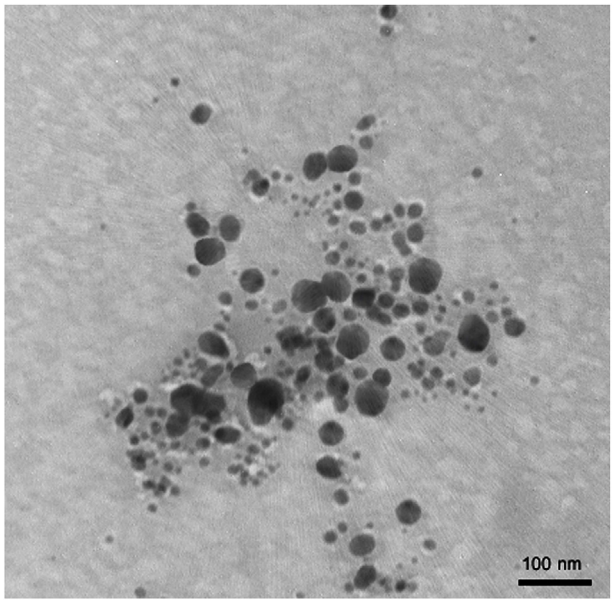

Fig. 5. TEM image of AgNPs. The spherical morphology of the nanoparticles is clear in the image.

metal ions by producing enzymes such as nitrate reductase. El-Batal et al. found that nitrate reductase enzymes existing in the culture supernatant of *Bacillus stearothermophilus* play an important role in the reduction of silver ions and formation of AgNPs (El-Batal et al., 2013; Wang et al., 2018).

According to UV-Vis spectrophotometer results, one peak was observed at 443 nm, which indicated the presence of AgNPs in the final colloid. There was no difference in the UV-Vis spectrum of the solution after 3 months, indicating the high stability of these nanoparticles. It seems that the presence of secreted proteins in bacterial supernatant contributes to the stability of synthesized nanoparticles (Nayak et al., 2016; Shankar et al., 2003). It is proven that proteins can bind to nanoparticles as stabilizers either through their free amine groups or cysteine residues (Khorrami et al., 2018; Vinoj et al., 2015). Capping proteins and other organic compounds prevent agglomeration of nanoparticles and are responsible for forming highly stable silver nanoparticles.

The FE-SEM results showed that the average size of these spherical nanoparticles was 45 nm. Previously, it had been found that AgNPs synthesized by various microorganisms have different sizes and shapes. According to some evidences, AgNPs produced by different strains of *Bacillus* mainly had spherical shapes, but different sizes ranging from 4 to 94 nm (Das et al., 2014; Ganesh Babu and Gunasekaran, 2009; Pourali and Yahyaei, 2016; Sathiyanarayanan et al., 2013).

Several unidentified crystalline peaks were observed in XRD spectrum, which might be because of the crystallization of bioorganic compounds on the surface of AgNPs (Anjum and Abbasi, 2016; Kalishwaralal et al., 2010b; Nayak et al., 2016). Besides, the energy-dispersive X-ray spectroscopy (EDS) results (Fig. 4,b) confirmed the XRD results.

Based on the evidences, AgNPs antibacterial activity against *E. coli* strain (19.7 mm) is more than the others, and *E. faecali* is a more resistant strain to AgNPs (16.2 mm) than other bacterial strains. The MIC and MBC results showed that AgNPs synthesized by the isolated strain had both inhibitory and killing effects on tested pathogenic strains. Similar results demonstrated that AgNPs produced by microorganisms had a broad range of antimicrobial effects on gram-positive and gram-negative bacteria (Barros et al., 2018; Ebrahimipour et al., 2017; Kushwaha et al., 2015; Levard et al., 2013; Nanda and Saravanan, 2009; Paul and Sinha, 2014; Pourali and Yahyaei, 2016). Although the mechanism of AgNPs antimicrobial activity has not been completely known, researchers believe that AgNPs possibly adhere to extracellular proteins and damage cells by creating pores in cell membrane, disrupting respiration function, interfering with DNA replications, and forming reactive oxygen species (ROS) such as hydrogen peroxide, superoxide anions, and hydroxyl radicals (Khorrami et al., 2018; Shanthi et al., 2016; Singh et al., 2016). Results of a research recently published

Table 1
Inhibition Zone Diameter, MIC, MBC and the concentration of AgNPs required to 100% inhibition of biofilm formation (IBF) against pathogenic bacteria. (Values of AgNPs are μg/mL).

IBF (μg/mL)	MBC (μg/mL)	MIC (μg/mL)	Inhibition Zone Diameter (mm) (Mean ± SD)	Pathogenic strains
3.125	25	12.5	18 ± 1.15	*K. pneumoniae PTCC1053*
3.125	12.5	6.25	19.7 ± 0.58	*E. coli O157:H7*
3.125	12.5	6.25	17.7 ± 0.58	*P. aeruginosa PTCC 1310*
15.3	12.5	6.25	17.3 ± 0.58	*L. monocytogenes PTCC 1298*
6.25	25	12.5	16.2 ± 0.29	*E. faecalis PTCC1237*
3.125	12.5	6.26	18.7 ± 1.5	*S. aureus PTCC 1112*

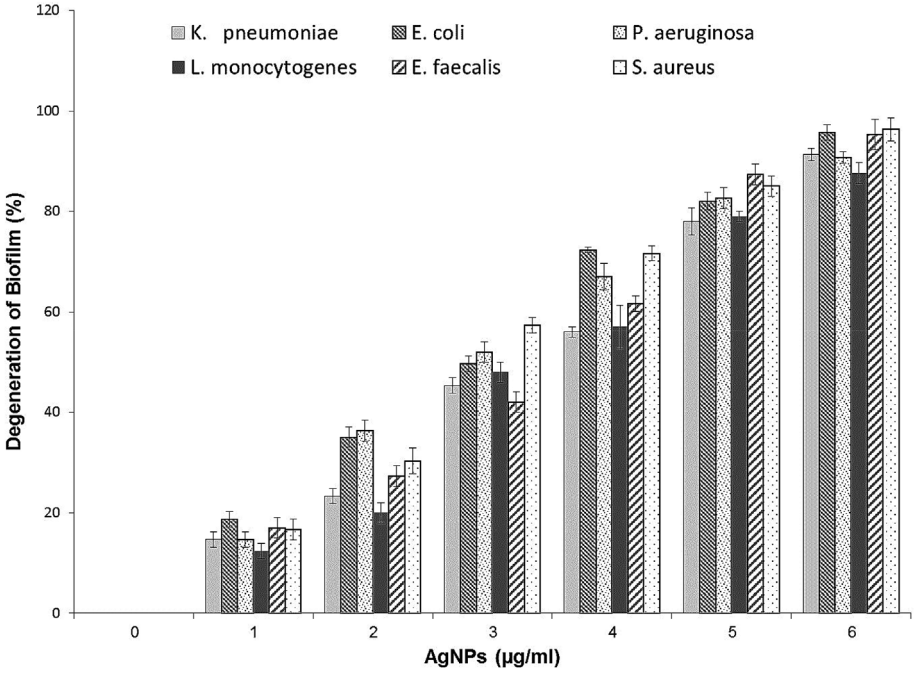

Fig. 6. Pathogenic bacteria biofilm degeneration by AgNPs (PBS was used as a control).

by Khorrami et al. show that *S. aureus* and *P. aeruginosa* bacterial strain synthesize beta-carotene and phenazine pigments, respectively, to counter the ROS resulted from silver nanoparticles (Khorrami et al., 2018).

It has already become clear that biofilm formation by pathogens on different surfaces has an important role in chronic and recurrent diseases. Therefore, inhibiting the formation of these structures or removing them is highly important (Singh et al., 2015). This study revealed that biosynthesized AgNPs using isolated *Bacillus thuringiensis* not only inhibited the formation of biofilm, but were also able to interfere in biofilm metabolic activity and its degradation. Besides, with increasing concentrations of AgNPs, degeneration of bacterial biofilm also increased so that the highest rate of bacterial biofilm degeneration (> 90%) was observed at 6 µg/mL concentration. It has already been reported that the inhibition of biofilm formation in some bacteria strain including *E. coli, P. aeruginosa, S. aureus* and *V. parahaemolyticus* Dav1, is directly dependent on NPs concentration. Kalishwaralal et al. have similarly reported anti-biofilm activity of bio-synthesized AgNPs and found that 100 nM of AgNPs resulted in a 95%–98% reduction in biofilm formation (Kalishwaralal et al., 2010a).

It seems that inhibition of biofilm formation by AgNPs is apparently due to the inhibition of exopolysaccharides synthesis in pathogenic

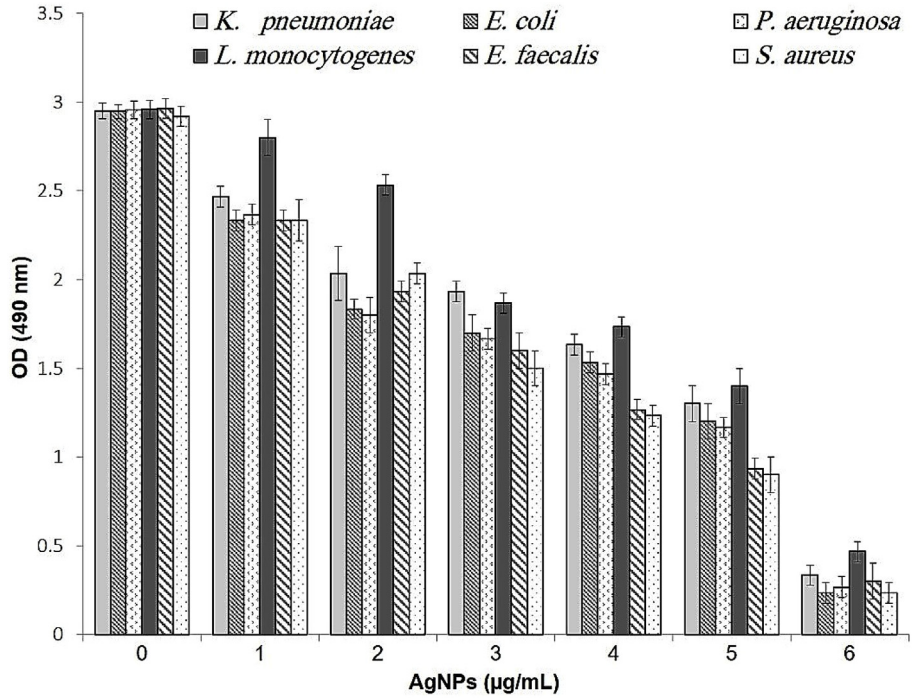

Fig. 7. Biofilm metabolic inhibition activity of AgNPs (decreasing in OD indicates the inhibition of the metabolic activity of biofilm).

bacteria (Radzig et al., 2013; Shanthi et al., 2016; Singh et al., 2016). Ansari et al. demonstrated that *S. aureus* and 10 of *S. epidermidis* bacterial colonies were grown, as crystalline black colonies, indicating the production of exopolysaccharides, which is a substrate for the synthesis of biofilm. However, the organisms did not survive when they were exposed to AgNPs. Thus, when the exopolysaccharide synthesis is blocked, the organisms cannot form the biofilm (Ansari et al., 2015; Stewart and Franklin, 2008). It is worth mentioning that different mechanisms might be involved in cell survival and biofilm formation; for example, Chaudhari et al. suggested that AgNPs might be involved in neutralizing adhesive substances thus preventing biofilm formation (Chaudhari et al., 2012; Gurunathan et al., 2014).

The results of biofilm metabolic activity assessments indicated that AgNPs synthesized by strain GL22, *Bacillus thuringiensis*, had the most inhibition effect on dehydrogenase enzyme activity at 6 µg/mL concentration. Crystal violet staining is the conventional method for studying the bacterial biofilm, but it is suggested that the results obtained from only crystal violet staining might be misleading because of nonspecific staining. Pitts et al. announced that crystal violet is useful to measure the biofilm amount, but not suitable for studying cell activity (Pitts et al., 2003). Thus, other techniques like cell counting technique along with this method should be used, leading to an increase in the cost and time of the study (Brown et al., 2013). Furthermore, the metabolic activity of biofilm's survived bacteria can be detected by measuring cell respiration and dehydrogenase enzyme activity using respiratory dye, and triphenyl tetrazolium chloride (TTC) (Mahdavi et al., 2007). Using TTC staining, Reuter et al. showed that viable cells collaborate with the adherent cell population in biofilm in aerobic conditions, and can recover from this biofilm (Reuter et al., 2010).

5. Conclusion

The present study reports identification of a novel strain of *Bacillus thuringiensis* isolated from the mine soil. Also, potential of the strain in the biosynthesis of silver nanoparticles has been examined. Based on the results, the strain is very robust in the biosynthesis of spherical silver nanoparticles with an average size of 42 nm. These nanoparticles not only inhibit the formation of bacterial biofilm but are also able to destroy pre-formed biofilm. On the other hand, they inhibit recovering of the bacterial structure by reducing the number of live cells in the biofilm. Therefore, the silver nanoparticles synthesized using *B. thuringiensis* strain can be used in the biomedical applications to controlling bacterial biofilm formation regarding their high anti-biofilm and antibacterial properties.

References

Abd El-Aziz, Abeer R.M., Al sohaibani, Saleh A., Mahmoud, Mohamed A., Sayed, Shaban R.M., A.O, M.R., 2012. Extracellular biosynthesis and characterization of silver nanoparticles using *Aspergillus niger* isolated from Saudi Arabia (strain Ksu-12). Dig J Nanomater Bios 7, 1491–1499.

Anjum, S., Abbasi, B.H., 2016. Thidiazuron-enhanced biosynthesis and antimicrobial efficacy of silver nanoparticles via improving phytochemical reducing potential in callus culture of *Linum usitatissimum* L. Int. J. Nanomed. 11, 715–728. https://doi.org/10.2147/IJN.S102359.

Ansari, M.A., Khan, H.M., Khan, A.A., Cameotra, S.S., Alzohairy, M.A., 2015. Anti-biofilm efficacy of silver nanoparticles against MRSA and MRSE isolated from wounds in a tertiary care hospital. Indian J. Med. Microbiol. 33, 101. https://doi.org/10.4103/0255-0857.148402.

Babu, J., Blair, C., Jacob, S., Itzhak, O., 2012. Inhibition of Streptococcus gordonii metabolic activity in biofilm by cranberry juice high-molecular-weight component. J. Biomed. Biotechnol. 2012, 1–7. https://doi.org/10.1155/2012/590384.

Bai, J.R., Zhong, K., Wu, Y.P., Elena, G., Gao, H., 2019. Antibiofilm activity of shikimic acid against Staphylococcus aureus. Food Control 95, 327–333. https://doi.org/10.1016/j.foodcont.2018.08.020.

Balouiri, M., Sadiki, M., Ibnsouda, S.K., 2016. Methods for in vitro evaluating antimicrobial activity: a review. J. Pharm. Anal. 6, 71–79. https://doi.org/10.1016/j.jpha.2015.11.005.

Barros, C., Fulaz, S., Stanisic, D., Tasic, L., 2018. Biogenic nanosilver against multidrug-resistant bacteria (MDRB). Antibiotics 7, 69. https://doi.org/10.3390/antibiotics7030069.

Brown, H.L., van Vliet, A.H.M., Betts, R.P., Reuter, M., 2013. Tetrazolium reduction allows assessment of biofilm formation by Campylobacter jejuni in a food matrix model. J. Appl. Microbiol. 115, 1212–1221. https://doi.org/10.1111/jam.12316.

Chaudhari, P.R., Masurkar, S.A., Shidore, V.B., Kamble, S.P., 2012. Effect of biosynthesized silver nanoparticles on Staphylococcus aureus biofilm quenching and prevention of biofilm formation. Nano-Micro Lett. 4, 34–39. https://doi.org/10.1007/BF03353689.

Das, V.L., Thomas, R., Varghese, R.T., Soniya, E.V., Mathew, J., Radhakrishnan, E.K., 2014. Extracellular synthesis of silver nanoparticles by the Bacillus strain CS 11 isolated from industrialized area. 3 Biotech 4, 121–126. https://doi.org/10.1007/s13205-013-0130-8.

Deljou, A., Goudarzi, S., 2016. Green extracellular synthesis of the silver nanoparticles using thermophilic Bacillus Sp. AZ1 and its antimicrobial activity against Several human pathogenetic bacteria. Iran. J. Biotechnol. 14, 25–32. https://doi.org/10.15171/ijb.1259.

Dufour, D., Leung, V., Lévesque, C.M., 2012. Bacterial biofilm: structure, function, and antimicrobial resistance. Endod. Top. 22, 2–16. https://doi.org/10.1111/j.1601-1546.2012.00277.x.

Ebrahimipour, S.Y., Machura, B., Mohamadi, M., Khaleghi, M., 2017. A novel cationic cobalt (III) Schiff base complex: preparation, crystal structure, Hirshfeld surface analysis, antimicrobial activities and molecular docking. Microb. Pathog. 113, 160–167. https://doi.org/10.1016/j.micpath.2017.10.034.

El-Batal, A.I., Amin, M.A., Shehata, M.M.K., Hallol, M.M.A., 2013. Synthesis of silver nanoparticles by Bacillus stearothermophilus using gamma radiation and their antimicrobial activity. World Appl. Sci. J. 22, 1–16. https://doi.org/10.5829/idosi.wasj.2013.22.01.2956.

Ganesh Babu, M.M., Gunasekaran, P., 2009. Production and structural characterization of crystalline silver nanoparticles from Bacillus cereus isolate. Colloids Surfaces B Biointerfaces 74, 191–195. https://doi.org/10.1016/j.colsurfb.2009.07.016.

Gurunathan, S., Han, J.W., Kwon, D.N., Kim, J.H., 2014. Enhanced antibacterial and antibiofilm activities of silver nanoparticles against Gram-negative and Gram-positive bacteria. Nanoscale Res. Lett. 9, 1–17. https://doi.org/10.1186/1556-276X-9-373.

Kalishwaralal, K., BarathManiKanth, S., Pandian, S.R.K., Deepak, V., Gurunathan, S., 2010a. Silver nanoparticles impede the biofilm formation by Pseudomonas aeruginosa and Staphylococcus epidermidis. Colloids Surfaces B Biointerfaces 79, 340–344. https://doi.org/10.1016/j.colsurfb.2010.04.014.

Kalishwaralal, K., Deepak, V., Ram Kumar Pandian, S.B., Kottaisamy, M., BarathManiKanth, S., Kartikeyan, B., Gurunathan, S., 2010b. Biosynthesis of silver and gold nanoparticles using Brevibacterium casei. Colloids Surfaces B Biointerfaces 77, 257–262. https://doi.org/10.1016/j.colsurfb.2010.02.007.

Khorrami, S., Zarrabi, A., Khaleghi, M., Danaei, M., Mozafari, M., 2018. Selective cytotoxicity of green synthesized silver nanoparticles against the MCF-7 tumor cell line and their enhanced antioxidant and antimicrobial properties. Int. J. Nanomed. 13, 8013–8024. https://doi.org/10.2147/IJN.S189295.

Kushwaha, A., Singh, V.K., Bhartariya, J., Singh, P., Yasmeen, K., 2015. Isolation and identification of E. coli bacteria for the synthesis of silver nanoparticles : characterization of the particles and study of antibacterial activity. Eur. J. Exp. Biol. 5, 65–70.

Levard, C., Mitra, S., Yang, T., Jew, A.D., Badireddy, A.R., Lowry, G.V., Brown Jr., G.E., 2013. Effect of chloride on the dissolution rate of silver nanoparticles and toxicity to E. coli. Environ. Sci. Technol. 47, 5738–5745. https://doi.org/10.1021/es400396f.

Mahdavi, M., Jalali, M., Kermanshahi, R.K., 2007. The effect of nisin on biofilm forming foodborne bacteria using microtiter plate method. Res. Pharm. Sci. 2, 113–118.

Mostaghasi, E., Zarepour, A., Zarrabi, A., 2018. Folic acid armed Fe3O4-HPG nanoparticles as a safe nano vehicle for biomedical theranostics. J. Taiwan Inst. Chem. Eng. 82, 33–41. https://doi.org/10.1016/j.jtice.2017.11.004.

Nanda, A., Saravanan, M., 2009. Biosynthesis of silver nanoparticles from Staphylococcus aureus and its antimicrobial activity against MRSA and MRSE. Nanomed. Nanotechnol. Biol. Med. 5, 452–456. https://doi.org/10.1016/j.nano.2009.01.012.

Natarajan, K., Selvaraj, S., Murty, V.R., 2010. Microbial production of silver nanoparticles. Dig. J. Nanomater. Biostructures 5, 135–140. https://doi.org/10.1016/j.colsurfa.2010.12.047.

Nayak, D., Ashe, S., Rauta, P.R., Kumari, M., Nayak, B., 2016. Bark extract mediated green synthesis of silver nanoparticles: evaluation of antimicrobial activity and antiproliferative response against osteosarcoma. Mater. Sci. Eng. C 58, 44–52. https://doi.org/10.1016/j.msec.2015.08.022.

Nithya, R., Ragunathan, R., 2009. Synthesis of silver nanoparticle using Pleurotus sajor caju and its antimicrobial study. Dig. J. Nanomater. Biostructures 4, 623–629.

Paul, D., Sinha, S.N., 2014. Extracellular synthesis of silver nanoparticles using *Pseudomonas aeruginosa* KUPSB12 and its antibacterial activity. Jordan J. Biol. Sci. 7, 245–250. https://doi.org/10.1007/s13204-013-0269-y.

Pitts, B., Hamilton, M.A., Zelver, N., Stewart, P.S., 2003. A microtiter-plate screening method for biofilm disinfection and removal. J. Microbiol. Methods 54, 269–276. https://doi.org/10.1016/S0167-7012(03)00034-4.

Pourali, P., Yahyaei, B., 2016. Biological production of silver nanoparticles by soil isolated bacteria and preliminary study of their cytotoxicity and cutaneous wound healing efficiency in rat. J. Trace Elem. Med. Biol. 34, 22–31. https://doi.org/10.1016/j.jtemb.2015.11.004.

Prasad, K., Jha, A.K., Kulkarni, A.R., 2007. Lactobacillus assisted synthesis of titanium nanoparticles. Nanoscale Res. Lett. 2, 248–250. https://doi.org/10.1007/s11671-007-9060-x.

Radzig, M.A., Nadtochenko, V.A., Koksharova, O.A., Kiwi, J., Lipasova, V.A., Khmel, I.A., 2013. Antibacterial effects of silver nanoparticles on gram-negative bacteria: influence on the growth and biofilms formation, mechanisms of action. Colloids Surfaces B Biointerfaces 102, 300–306. https://doi.org/10.1016/j.colsurfb.2012.07.039.

Reuter, M., Mallett, A., Pearson, B.M., Van Vliet, A.H.M., 2010. Biofilm formation by Campylobacter jejuni is increased under aerobic conditions. Appl. Environ.

Microbiol. 76, 2122–2128. https://doi.org/10.1128/AEM.01878-09.
Sathiyanarayanan, G., Seghal Kiran, G., Selvin, J., 2013. Synthesis of silver nanoparticles by polysaccharide bioflocculant produced from marine Bacillus subtilis MSBN17. Colloids Surfaces B Biointerfaces 102, 13–20. https://doi.org/10.1016/j.colsurfb.2012.07.032.
Shahverdi, A.R., Minaeian, S., Shahverdi, H.R., Jamalifar, H., Nohi, A.A., 2007. Rapid synthesis of silver nanoparticles using culture supernatants of Enterobacteria: a novel biological approach. Process Biochem. 42, 919–923. https://doi.org/10.1016/j.procbio.2007.02.005.
Shankar, S.S., Ahmad, A., Sastry, M., 2003. Geranium leaf assisted biosynthesis of silver nanoparticles. Biotechnol. Prog. 19, 1627–1631. https://doi.org/10.1021/bp034070w.
Shanthi, S., David, B., Velusamy, P., Vijayakumar, S., Ta, C., Vaseeharan, B., 2016. Microbial Pathogenesis Biosynthesis of silver nanoparticles using a probiotic Bacillus licheniformis Dahb1 and their antibio film activity and toxicity effects in Ceriodaphnia cornuta. Microb. Pathog. 93, 70–77. https://doi.org/10.1016/j.micpath.2016.01.014.
Singh, P., Singh, H., Kim, Y.J., Mathiyalagan, R., Wang, C., Yang, D.C., 2016. Extracellular synthesis of silver and gold nanoparticles by Sporosarcina koreensis DC4 and their biological applications. Enzym. Microb. Technol. 86, 75–83. https://doi.org/10.1016/j.enzmictec.2016.02.005.
Singh, R., Shedbalkar, U.U., Wadhwani, S.A., Chopade, B.A., 2015. Bacteriagenic silver nanoparticles: synthesis, mechanism, and applications. Appl. Microbiol. Biotechnol. 99, 4579–4593. https://doi.org/10.1007/s00253-015-6622-1.
Sonak, S., Bhosle, N.B., 1995. A simple method to assess bacterial attachment to surfaces. Biofouling 9, 31–38. https://doi.org/10.1080/08927019509378289.
Stepanovic, S., Vukovic, D., Hola, V., Bonaventura, G. Di, Djukic´, S., Irkovic´, I.C., Ruzicka, F., 2007. Quantification of biofilm in microtiter plates: overview of testing conditions and practical recommendations for assessment of biofilm production by Staphylococci. Apmis 115, 891–899. https://doi.org/10.1111/j.1600-0463.2007.apm_630.x.
Stewart, P.S., Franklin, M.J., 2008. Physiological heterogeneity in biofilms. Nat. Rev. Microbiol. 6, 199. https://doi.org/10.1038/nrmicro1838.
Suresh, Y., Annapurna, S., Singh, A.K., Chetana, A., Pasha, C., Bhikshamaiah, G., 2016. Characterization and evaluation of anti-biofilm effect of green synthesized copper nanoparticles. Mater. Today Proc. 3, 1678–1685. https://doi.org/10.1016/j.matpr.2016.04.059.
Tamura, K., Dudley, J., Nei, M., Kumar, S., 2007. MEGA4: molecular evolutionary Genetics analysis (MEGA) software version 4.0. Mol. Biol. Evol. 24, 1596–1599. https://doi.org/10.1093/molbev/msm092.
Vinoj, G., Pati, R., Sonawane, A., Vaseeharan, B., 2015. In vitro cytotoxic effects of gold nanoparticles coated with functional acyl homoserine lactone lactonase protein from Bacillus licheniformis and their antibiofilm activity against proteus species. Antimicrob. Agents Chemother. 59, 763–771. https://doi.org/10.1128/AAC.03047-14.
Wang, L., Zhang, H., Rehman, M.U., Mehmood, K., Jiang, X., Iqbal, M., Tong, X., Gao, X., Li, J., 2018. Antibacterial activity of Lactobacillus plantarum isolated from Tibetan yaks. Microb. Pathog. 115, 293–298. https://doi.org/10.1016/j.micpath.2017.12.077.
Yahyaei, B., Pourali, P., 2017. An alternative method for biological production of silver and gold nanoparticles. Int. J. Microbiol. Res. Rev. 6, 230–235.